Available online at www.sciencedirect.com

ScienceDirect

Ceramics International 40 (2014) 3469–3475

CERAMICS INTERNATIONAL

www.elsevier.com/locate/ceramint

# TPR studies on NiO–CGO composites prepared by combustion synthesis

J. Marrero-Jerez[a], E. Chinarro[b], B. Moreno[b], M.T. Colomer[b], J.R. Jurado[c], P. Núñez[a,*]

[a]*Departamento de Química Inorgánica, Universidad de La Laguna, 38200 San Cristóbal de La Laguna, Tenerife, Spain*
[b]*Instituto de Cerámica y vidrio (ICV), CSIC, C/Kelsen 5, Campus de Cantoblanco UAM, 28049 Madrid, Spain*
[c]*Instituto de Productos Naturales y Agrobiología (IPNA), CSIC, Avda. Astrofísico Francisco Sánchez, 38206 San Cristóbal de La Laguna, Tenerife, Spain*

Received 17 January 2013; received in revised form 17 September 2013; accepted 18 September 2013
Available online 1 October 2013

**Abstract**

NiO–ceria composites, which are promising candidates as anodes for intermediate temperature solid oxide fuel cells (IT-SOFCs) were prepared by urea combustion synthesis (UCS) method. The UCS method is, in general, a highly suitable synthesis method for the production, at low temperatures, of fine and reactive powders. By means of XRD and SEM-EDX techniques, the structural, microstructural and compositional behavior of the as-prepared powders has been studied. In addition, temperature programmed reduction (TPR) tests were performed to investigate the reducibility of the composites. After reduction of the NiO–CGO as-prepared compositions, the combustion powders exhibit the presence of Ni, the fluorite CGO solid solution that remains stable and NiO is no longer present. The morphology and size of the nanoparticles and aggregates of the as-prepared powders make them reactive at intermediate temperatures (400–800 °C). TPR tests show wide overlapping peaks which are associated with the two primary reduction stages; one is related to the surface NiO reduction mechanism and the other to the coexistence of interactions between the NiO–CGO surface and bulk reduction processes. Further, after TPR measurements the resulting products have high phase stability and reproducibility.


*Keywords:* Ceria; Nickel oxide; Anode; TPR; SOFC

## 1. Introduction

In recent years, most of the efforts in SOFC development have focussed on intermediate temperature solid oxide fuel cells (IT-SOFCs), often using YSZ and/or CGO as electrolytes [1–3]. For SOFC development, relatively high ionic conductivity of solid electrolytes is not the only requirement. At intermediate temperatures, ceria-based materials may have high enough ionic conductivity at temperatures as low as 600 °C, however they do not have suitable long term stability. YSZ with low thickness (less than 80 μm) is still more appropriate as an electrolyte candidate in SOFC devices [4].

Ni–Ceria based materials are also being considered for use as fuel anode electrodes for IT-SOFCs, even in devices where YSZ is used as the electrolyte [4,5]. Ni–CGO has been considered very effective in preventing coke build-up when using weakly humidified $CH_4$ fuels. This is due to the ability to transform carbon deposits into CO or $CO_2$ during or after $CH_4$ decomposition through the mobile bulk (lattice) oxygen. Thus, ceria has been used as the ceramic part in Ni- or Ru-cermet anodes [6]. Beneficial effects have been interpreted as being due to the enhancement of the length of the three phase boundary zones. Analyses of microstructure, phase stability, reduction behavior and electrical properties have been carried out on NiO–CGO composites [7]. These are essential factors if these materials are to be used as the anode component.

To date, there has been little research on the routes of synthesis of NiO ceria-doped cermets for IT-SOFC applications. Employed routes include hydrothermal synthesis [8], oxalate co-precipitation [9] and carbonate co-precipitation [10]. As it is well-known, these and other wet-chemical synthesis methods produce single or multicomponent oxide powders with high sinterability, large surface areas, well-defined chemical compositions and homogeneous distributions of the elements. However, in spite of the quality of the powders produced and

*Corresponding author. Tel.: +34 92 23 18501.
*E-mail address:* pnunez@ull.es (P. Núñez).

0272-8842/$ - see front matter © 2013 Elsevier Ltd and Techna Group S.r.l. All rights reserved.
http://dx.doi.org/10.1016/j.ceramint.2013.09.083

although powder synthesis can be achieved at low temperature, many solution processes are complicated and lengthy procedures which limit their applicability.

In the last decade, Wet Chemical Combustion Synthesis (using fuels such as urea, glycine, sucrose, etc) has been widely employed to obtain multicomponent ceramic oxides [11–13], phosphates [14], etc. These techniques have been gaining reputation as straightforward preparation processes which produce homogeneous, very fine, crystalline powders, in some cases in a single step, reducing the preparation time and without the need for intermediate decomposition and/or calcining steps [13]. The basis of the combustion synthesis technique comes from thermochemical concepts used in the field of propellants and explosives [15]. Exothermic heat released by the reaction causes the temperature to rise very fast and sustains it at the high level necessary for synthesis to occur (around 1000 °C depending on the raw materials). The large amount of evolved gases results in the formation of a foam whose structure is propagated as a wave along the oxide powder precursor. Because of the homogeneity of the raw materials solution and the high speed of the reaction, the resulting product is single phase and homogeneous. In general, the particles are very fine and the temperature reached is usually enough to promote their crystallization.

The aim of this investigation is to prepare NiO–CGO fine crystalline powders with high reactivity due to the size of their particles. Urea combustion synthesis (UCS), which is capable of producing very fine powders of different compounds in a one-pot synthesis was used. These ceramic composites were characterized by XRD and TPR studies.

## 2. Experimental

### 2.1. Powder synthesis

The ceria based ceramics were synthesized by combustion reactions employing hydrated salts, $Ce(NO_3)_3 \cdot 6H_2O$ (99.0%, Aldrich), $Gd(NO_3)_3 \cdot 6H_2O$ (99.9%, Aldrich), $Ni(NO_3)_3 \cdot 6H_2O$ (99.0%, Aldrich), as cation precursors; and urea, $CO(NH_2)_2$ (98.0%, Aldrich), was used as fuel.

Urea Combustion Synthesis (UCS) was used to prepare NiO–CGO composite powders in a one-step reaction. Stoichiometric amounts of $Ce(NO_3)_3 \cdot 6H_2O$ and $Gd(NO_3)_3 \cdot 6H_2O$, were taken in the ratio $CeO_2/Gd_2O_3$ 90% mol: 10% mol to obtain the CGO ($Ce_{0.82}Gd_{0.18}O_{1.91}$) solid solution as one component, and a stoichiometric amount of $Ni(NO_3)_3 \cdot 6H_2O$ was introduced as the second component to produce the NiO–CGO composite. The prepared compositions of NiO and CGO in the ratios NiO: CGO (mol/mol) of 35:65; 50:50 and 65:35.

Each mixture of stoichiometric compositions was calculated based on the total oxidizing and reducing valences of the oxidizer and the fuel, in order to release the necessary energy for the reaction. The reactants were first melted, in a wide-mouth vitreous silica vessel, by heating to 300 °C on a hot-plate inside a fume cupboard, under ventilation. Care must be taken during the decomposition as toxic gases such as $NO_x$ can be produced. The reaction lasted for less than 15 min and produced dry and very brittle foams, that readily crumbled into very fine powders, accompanied by a large increase in volume when compared to the original volume of liquid. Further details on the combustion reaction can be found elsewhere for other related systems [16].

### 2.2. TPR measurements

By means of Temperature-Programmed Reduction (TPR) tests, the number of reducible species in the Ni–CGO anodes was determined. The results reveal the temperatures at which the reduction takes place. The TPR analysis begins when a reducing gas is passed through the sample. While the gas is flowing, the temperature of the sample is increased linearly over time and hydrogen comsumption by adsorption and reduction is detected. Changes in concentration are determined by measuring the thermal conductivity of gas mixture products. This information yields the hydrogen uptake volume. The equipment is an AUTOCHEM II 2920, Automated Catalyst Characterisation System (Micromeritics).

100 mg of each sample was loaded on top of glass wool in a quartz tube inside an electric furnace. All samples were pretreated by heating in a helium atmosphere at 350 °C for one hour before the TPR tests in order to remove contaminants. After cooling to room temperature, reduction processes were carried out using a 20 ml $min^{-1}$ gas flow of 5 vol% $H_2$/Ar in the temperature range of 25–900 °C at a heating rate of 10 °C $min^{-1}$. Hydrogen consumption was monitored using an in-situ thermal conductivity detector (TCD). A cryogenic trap, consisting of a gel formed by adding liquid nitrogen to isopropyl alcohol in a dewar flask, was used to prevent water entering the detector.

### 2.3. Powder characterisation

In order to investigate the formation of the composites, room temperature X-ray diffraction patterns (XRD) were collected with a PANalytical X'Pert Pro automated diffractometer, equipped with a primary monochromator (Cu $K_{\alpha 1}$ radiation) and an X'Celerator detector. Scans were performed in the $2\theta$ range (15–100°) with 0.016° steps for 2 h. XRD data treatment was performed using WinPlotr suite software [17]. Phase identification was performed with X'Pert HighScore Plus v.2.2d software [18].

The specific surface area of the powders was determined via the BET method using MS-13 equipment from Quantachrome Corp. Particle size distributions of the samples after the reaction were analyzed using a Laser Pulse Analyser from Malvern (Mastersizer). SEM/EDS observations were performed using ZEISS-DSM 950 EDS equipment, and TEM/EDS observations with Hitachi H-7100, 125 kV equipment. These characterization techniques were used to determine surface morphology and to identify the nickel nano-particles of the Ni–CGO anode cermet. The particle size and crystallinity of the as-prepared powders produced in the stoichiometric reactions were also investigated by TEM.

The as-prepared powders were analyzed by Inductively Coupled Plasma-Optical Emission Spectrometry (ICP-OES, Iris Advantage, Thermo Jarrel-Ash, USA) in order to determine the concentration of soluble species. The error in the ICP-OES measurements was below 1% of measured value. The average of three measurements is always given.

## 3. Results and discussion

### 3.1. Synthesis and thermochemical response

The combustion reaction was fast and intense and the resulting as-prepared powders were dry and homogeneous foams. The reaction is quite efficient and produces the whole composite, in just a one-pot synthesis. The overall synthesis reaction can be written as:

$$(1-x)Ni(NO_3)_2\cdot 6H_2O(s)+0.82xCe(NO_3)_3\cdot 6H_2O(s)+0.18xGd(NO_3)_3\cdot 6H_2O(s)+mCO(NH_2)_2(s)+(1.5\ m-1.045x-2.5)O_2(g)\Rightarrow(1-x)NiO+xCe_{0.82}Gd_{0.18}O_{1.91}+(6+2\ m)H_2O(g)+(1+0.5x+m)N_2(g)+mCO_2(g)$$

Applying thermochemical concepts from propellant chemistry to this synthesis, the total summatory of the products of the cation and anion valences by the stoichiometric coefficients should be zero (Eq. (1)).

$$\sum oxidant\ element\ coefficients\times Valences+\sum reductor\ element\ coefficients\times Valences=0 \quad (1)$$

For the calculation, the following final state valences were assumed: C(+4); O(−2); H(+1); N(0); Ni(+2); Gd(+3) and Ce(+4). These valences should be balanced by the total valences of the fuel; thus the stoichiometric composition of the redox mixture, in order to release the maximum energy for the reaction, demands that $m=2.12$, 2.01 or 1.91 mol of urea for $x=0.65$, 0.5 or 0.35 respectively (being $m=(10+4.18x)/6$).

According to the literature [12,13,16], the temperature reached locally during the combustion is higher than 800 °C, a temperature that allows the formation of the composite.

Using stoichiometric molar compositions of the mixtures, NiO–CGO composites were produced. The reactions were fast and produced smooth dry green foams, accompanied by a large increase in volume when compared to the original volume of liquid. Typical densities of these soft foams (readily transformed into powder merely by handling), calculated based on their geometry, are 102 kg/m$^3$ for NiO+CGO.

### 3.2. Powder morphology studies

The morphology and the particle size of the as-prepared powders produced in the stoichiometric reactions were investigated by TEM. Fig. 1 shows a TEM micrograph of the 65 mol% NiO–CGO sample powders, where aggregates of very fine crystals could be seen. As it is expected, BET measurements of this material (65 mol% NiO–CGO) show a decreasing in the specific surface area from the as prepared powders (28 m$^2$/g) to the reduced powders (14 m$^2$/g) due to redox changes in the material combined with the grain's growth, due to sample heating at high temperature in this process. Typical powder morphologies of the stoichiometric as-prepared powders can be observed in the back scattering SEM image (Fig. 2). NiO and CGO can be identified in Fig. 2, due their different electronic densities, corresponding the gray part to NiO and the white grains to CGO ceramic, and a homogeneous distribution in between can be observed. Using EDX (Fig. 2), no silica or other contaminants were observed, which indicates that this method can be used to obtain very pure powders. The final silica content was determined by Inductively Coupled Plasma Chemical (ICP) analysis and was found to be 150 ppm, dispersed and easy to control.

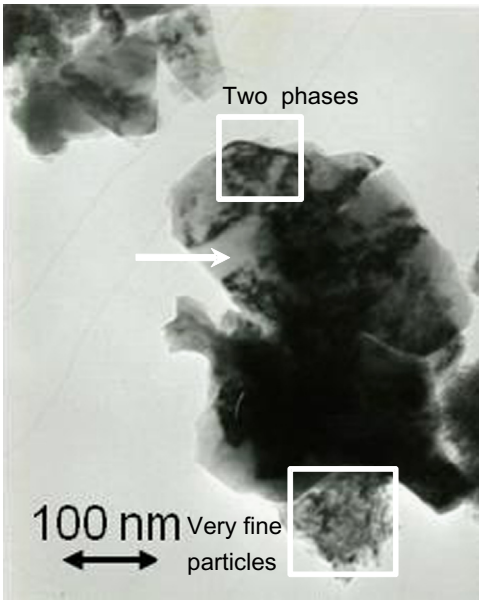


Fig. 1. TEM micrograph of the stoichiometric as-prepared 65 mol% NiO–CGO sample.

The XRD patterns of NiO–CGO as-prepared powders showed nano crystalline powders of fluorite phase with additional Bragg peaks of the NiO phase (Fig. 3). Similar results were obtained by Chavan et al. [5]. From the X-ray diffraction patterns of the as-prepared powders it can be seen that the combustion reactions were achieved in a single step. This demonstrates that the urea combustion reaction is extremely exothermic providing the necessary heat for the synthesis reactions from the metallic nitrates as precursors and giving rise to submicrometric powders.

In this case, the temperature is high enough to promote synthesis of the solid solution CGO with the ceria fluorite structure from metallic nitrates, with $CeO_2$ and/or $Gd_2O_3$ no longer reaction products. As mentioned before, the amount of silica is low and well controlled, and uniformly dispersed. Using XRD it can be observed that there are neither other phases nor any significant reaction products such as carbonates or residual precursor or at least at levels lower than the thresholds of this technique. Only a small Bragg peak of Ni for the sample with higher content of NiO (35% CGO–65% NiO)

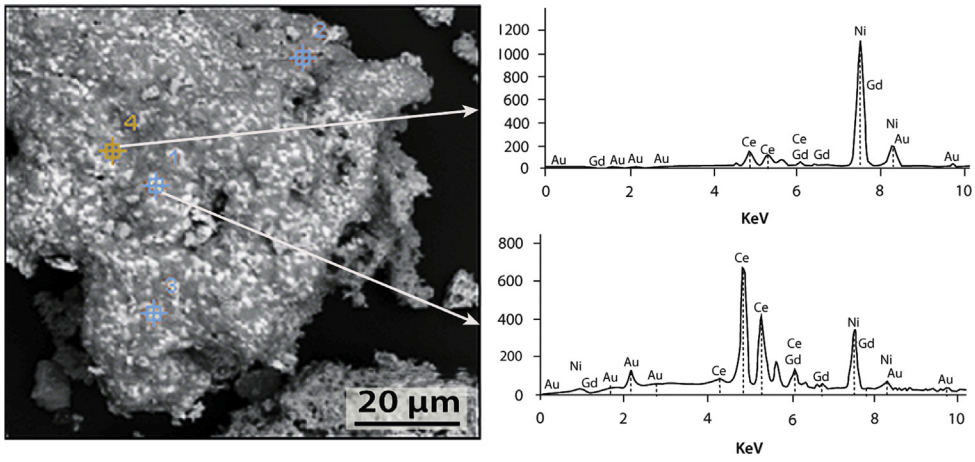


Fig. 2. Back scattering SEM micrograph (left image) and EDX spectra (right side) of the 65 mol% NiO–CGO as-prepared sample. CGO and NiO can be identified as white and gray grains respectively.

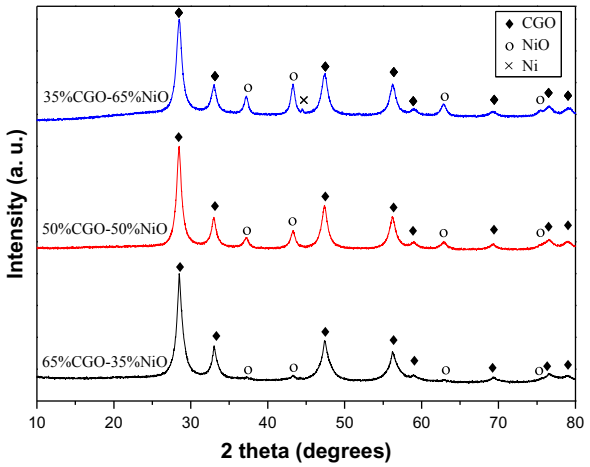


Fig. 3. XRD of NiO–CGO as-prepared composites with different amounts of NiO.

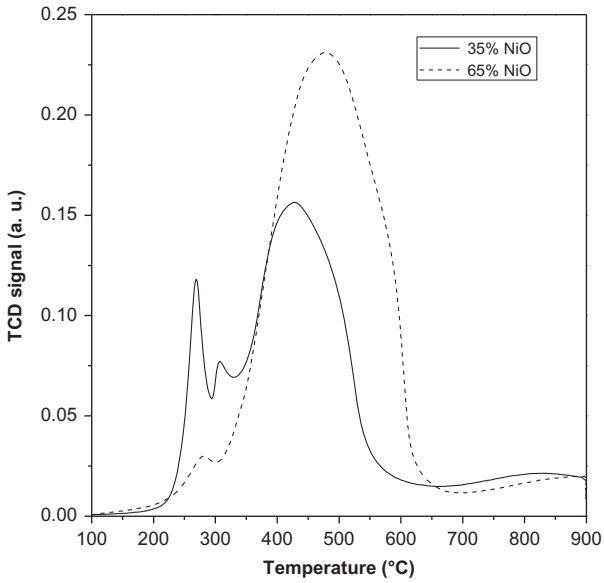


Fig. 4. TPR measurements of the NiO–CGO as-prepared samples.

was observed. This fact confirms that a reduction atmosphere is produced locally during the combustion.

### 3.3. Reduction behavior

As-prepared samples were studied using TPR and certain impurities remain in these samples, as shown in Fig. 4. Peaks at very low temperatures (200–300 °C) are associated with either adsorbed oxygen [19], or residual species not well eliminated during the combustion synthesis. Due to these impurities are normally in a small amount and prevailing amorphous they may not be detected by XRD. The time of combustion synthesis is short and therefore these residual species (i.e. nitrates, and carbonaceous species) could not be completely removed. According to data reported in the literature two main peaks are commonly found for similar CGO–NiO samples. Thus, the wide overlapping peak at lower temperatures can be assigned to the reduction of the distinct states of NiO species while the latter peak may be associated with reduction of the CGO support [19–23].

Fig. 4 shows the TPR of the 35 mol% NiO sample. In this case, four peaks are detected. Low temperature peaks, centered at 270 °C and 310 °C, are both associated with the aforementioned impurities. The third, a wide overlapping peak centered at 425 °C, can be ascribed to the surface and/or surface-bulk NiO reduction to Ni mechanisms and also to the different interactions between NiO particles and the CGO support [20,21]. Finally, the peak observed at high temperature (850 °C) is commonly ascribed to $CeO_2$ bulk reduction [19–23].

The sample with composition 65 mol% NiO–CGO exhibits a first peak at 280 °C, ascribed to impurities, a wide overlapping peak at 475 °C, related to reduction of the different NiO species, and a small peak corresponding to CGO reduction which is centered at 850 °C (Fig. 4).

Taking this into account, the as-prepared samples should be thermally pre-treated in order to remove their impurities, and therefore a calcination in air was performed at 900 °C for 2 h. Their XRD spectra can be seen in Fig. 5. As can be observed,

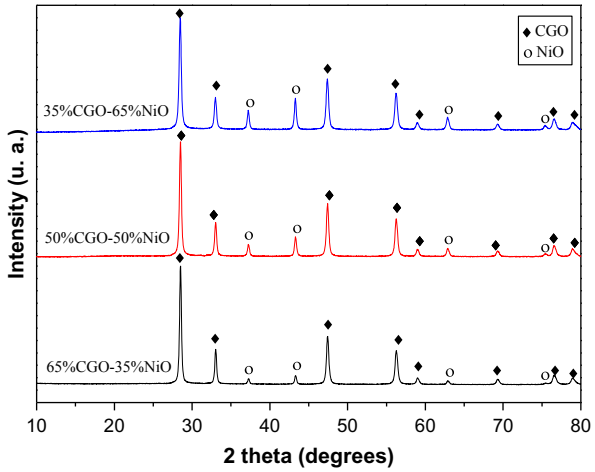


Fig. 5. XRD of 35, 50, 65 mol% NiO–CGO samples after calcination at 900°C/2 h in air.

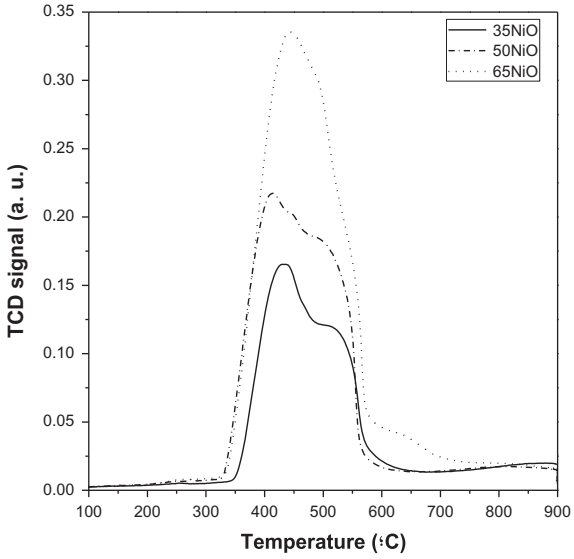


Fig. 6. TPR of CGO–NiO composites after calcination at 900°C/2 h in air.

CGO–NiO composites remain stable after calcination and neither impurities nor secondary phases were detected. After calcination of the powders at 900 °C, new TPR tests were performed. Results for three different CGO–NiO compositions are shown in Fig. 6.

For the 35 mol% NiO sample, a first overlapping peak at low temperatures (centered around 410 °C) can be observed. This overlapping peak can be de-convoluted into two peaks, the first peak is ascribed to the reduction of surface NiO particles which have less interaction with the CGO support, while the second peak observed (540 °C) is related to the NiO particles that have a higher interaction with the support [20,21]. The peak found at 850 °C corresponds to reduction of the CGO phase as mentioned before. In general, powder samples containing NiO, CGO, and/or NiO–CGO and prepared using different synthesis techniques show similar $H_2$-TPR profiles [19–22]. According to these authors, the $H_2$-TPR profile of the stand-alone NiO powder showed an overlapping reduction peak between 300 and 700 °C, whereas the $H_2$-TPR profile for NiO–CGO powder showed two distinct reduction peaks: a wide peak between 300 and 600 °C (reduction of NiO species) and another centered at 850 °C (reduction of the CGO support) [19–20].

Similar results are shown for 50 mol% NiO sample (Fig. 6). In this case the peaks are centered at 420 °C and 500 °C for the two main contributions to the NiO reduction species and around 850 °C for reduction of the bulk CGO support. In addition, it can be observed that when CGO content increases, a bigger separation between the NiO species peaks occurs. This fact indicates that ceria modifies the nature of the Ni-species [22].

For the 65 mol% NiO–CGO sample, four reduction overlapping peaks centered at 480, 540, 645 and 850 °C were observed in the $H_2$-TPR profile (Fig. 6). According to Shan et al., crystallized NiO, CGO–NiO solid solution and NiO highly dispersed on CGO co-exist for high nickel contents [19]. In this particular case, the peaks centered at 480 °C and 540 °C are associated with the reduction of NiO species with

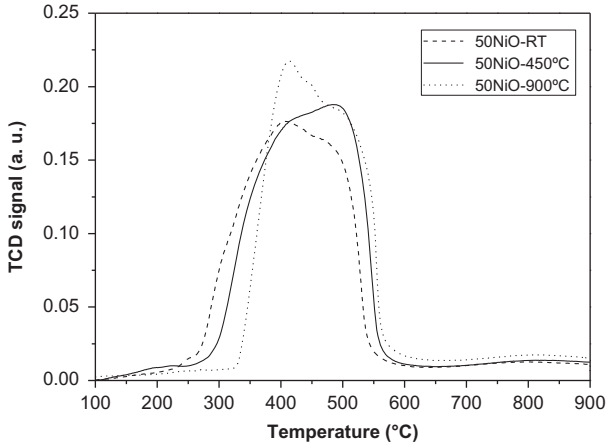


Fig. 7. TPR of CGO-50 mol% NiO composites at different calcination temperatures.

different interactions with CGO while the peak found at 645 °C may be attributed to the reduction of NiO–CGO solid solution. The last peak (850 °C) can be assigned to the bulk reduction of the CGO support. A slight shift towards higher temperatures in the TPR peak positions as well as an increase in peak area is observed as the NiO content increases. These findings are in good agreement with other authors [19,22].

In order to determine the influence of calcination temperature on the reduction behavior of the CGO–NiO cermets, different heat treatments and subsequent TPR tests were performed. As we can see in Fig. 7, the onset of the reducing process occurs at higher temperatures when calcination temperature is increased. TPR of the as-prepared sample shows that the overlapping peak associated with reduction of NiO species shows an onset at 250 °C whereas the sample calcined at 450 °C for 2 h starts its reducing process at 275 °C, and the one calcined at 900 °C begins at 340 °C. This fact is ascribed

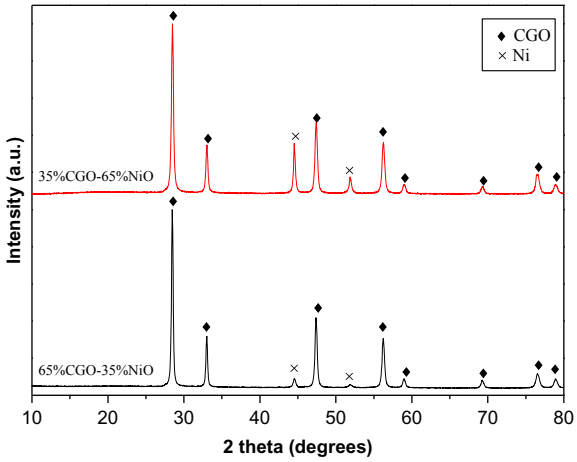


Fig. 8. XRD of 35 and 65 mol% NiO samples after TPR tests (performed up to 900 °C).

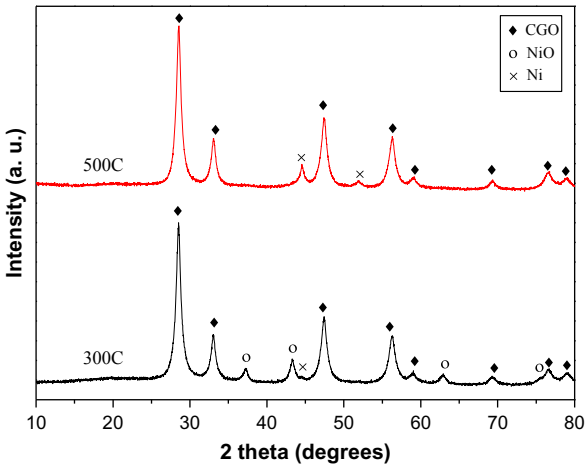


Fig. 9. XRD patterns for the 50 mol% NiO–CGO sample after half TPR tests (300 and 500 °C).

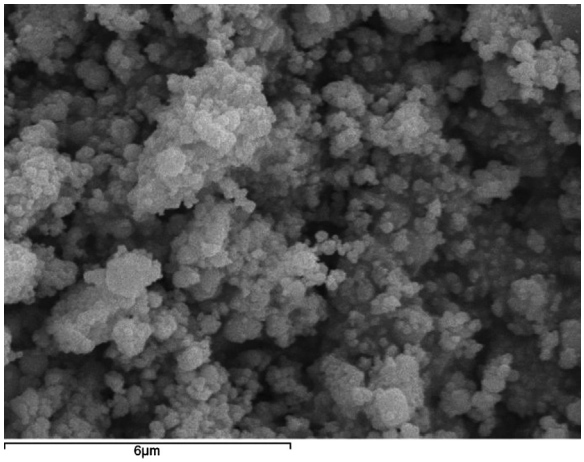


Fig. 10. SEM micrograph of 35 mol% NiO–CGO (900 °C) after TPR tests (900 °C).

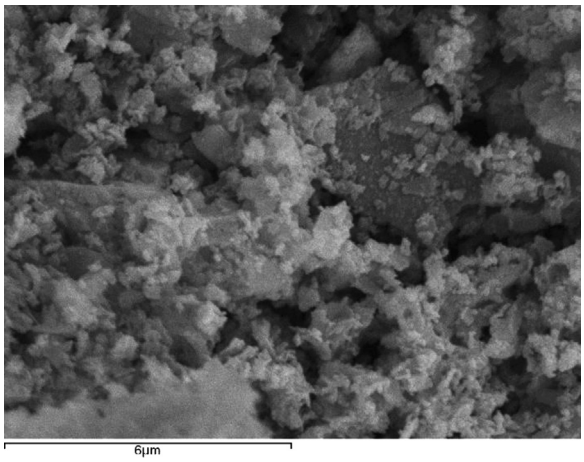


Fig. 11. SEM micrograph of 65 mol% NiO–CGO (900 °C) after TPR tests (900 °C).

to the increase in growth of NiO particles on the surface of ceria with increasing calcination temperatures. All samples showed the end of reduction of NiO species at around 600 °C as expected. As has been observed in previous results, the small peak associated with CGO bulk reduction is centered at 850 °C in all cases, thus no influence of calcination temperatures on CGO bulk reduction is observed.

The effect of TPR on the as-prepared samples is shown in Fig. 8. The XRD patterns confirm that after reduction due to the TPR tests all the as-prepared samples exhibit the presence of CGO and metallic Ni. NiO is no longer detected after reduction, thus complete reduction of NiO species to Ni is achieved. A relevant result is concerning the XRD 50 mol% NiO–CGO sample pattern shown in Fig. 9. In this case, the XRD pattern obtained when the sample was released from the reduction program at 300 °C showed three different phases. The Bragg peaks were indexed as metallic Ni (small amount) (PDF 01-087-0712), NiO (PDF 00-044-1159) and fluorite-type ceria (CGO) (PDF 01-075-0120). That means that the reduction process has started at 300 °C and NiO species have been partially reduced to metallic Ni at this temperature. In the sample treated at 500 °C, the XRD pattern showed only metallic Ni and flourite ceria phases so the reduction of NiO species takes place between 300 and 500 °C. This fact agrees well with the TPR results.

TPO experiments were performed after TPR, where oxygen consumption is observed. After these TPO tests XRD patterns were performed confirming the appearance of NiO and metal Ni was not observed. The NiO should be located on the surface of the CGO grain because the temperature of the TPO experiment is not high enough for the re-diffusion of NiO into the bulk.

Therefore, all the CGO–NiO composites studied in this work present good activity towards the oxidation of $H_2$ in the temperature range 300–600 °C (with a maximum around 450 °C) as TPR tests show. This fact is a promising result for the application of these materials as candidates for IT-SOFC anodes.

SEM micrographs in Figs. 10 and 11 show that the powder after the TPR tests consists of aggregates of particles of nanometric sizes, with the appearance of brittle foam coexisting with harder aggregates of larger grains of ~2 μm. In addition, EDX analysis

demonstrated that the as-prepared powders after TPR tests exhibit phase stability and reproducibility, confirming the results obtained previously using XRD.

## 4. Conclusions

The urea combustion synthesis method (UCS) has been revealed as a simple, fast and reliable route to synthesize these kinds of materials. The resulting submicrometric powders of the composite NiO–CGO can be highly controlled on both composition and homogeneity. After reduction of NiO–CGO as-prepared powders, TPR diagrams show three main peaks, two of them overlapping. After de-convolution, the two overlapping peaks representing the primary reduction steps can be ascribed as follows, the first to the reduction of well dispersed NiO species which interact weakly with CGO, and the second to NiO species with a strong interaction with CGO. The third, which is much smaller, is ascribed to the reduction of CGO. The TPR resulting products were shown to have high phase stability. All the tests were reproducible and have the same remaining phases. For as-prepared samples, peaks at very low temperatures (200–300 °C) are associated with either adsorbed oxygen or residual species not well eliminated during the combustion synthesis. These residual species are present due to the short-time reaction and may include nitrates, carbonates and other carbonaceous species, as amorphous materials, and therefore they were not detected by XRD. Also, TPR tests showed that the CGO–NiO composites studied in this work present good activity towards the oxidation of $H_2$ in the temperature range of 300–600 °C (with a maximum around 450 °C), which is a promising result for the application of these materials as candidates for IT-SOFC anodes.

## Acknowledgments

The research leading to these results has received funding from the European Union's Seventh Framework Program (FP7/2007-2013) for the Fuel Cells and Hydrogen Joint Technology Initiative under Grant agreement no.[245355] (ROBANODE). The authors are also grateful for financial support to the Spanish Government Research Program for Grants MAT2007-60127 and MAT2010-16007 (cofinanced by MICINN and FEDER funds) and one of us (J. M-J) for a pre-doctoral fellowship (FPI).

## References

[1] J.B. Goodenough, Y.H Huang, Alternative anode materials for solid oxide fuel cells, Journal of Power Sources 173 (2007) 1–10.
[2] E.V. Tsipis, V.V. Kharton, Electrode materials and reaction mechanisms in solid oxide fuel cells: a brief review, Journal of Solid State Electrochemistry 12 (2008) 13671391.
[3] T.J. Huang, C.H. Wang, Factors in forming CO and $CO_2$ over a cermet of Ni-gadolinia-doped ceria with relation to direct methane SOFCs, Journal of Power Sources 163 (2006) 309–315.
[4] N.P. Brandon, S. Skinner, B.C.H. Steele, Recent advances in materials for fuel cells, Annual Review of Materials Research 33 (2003) 183–213.
[5] A.U. Chavan, L.D. Jadhav, A.P. Jamale, S.P. Patil, C.H. Bhosale, S.R. Bhardwaj, P.S. Patil, Effect of variation of NiO on properties of NiO/GDC (gadolinium doped ceria) nano-composites, Ceramics International 38 (2012) 3191–3196.
[6] W. Huang, P. Shuk, M. Greenblatt, Hydrothermal synthesis and properties of terbium- or praseodymium-doped $Ce_{1-x}Sm_xO_{2-x/2}$ solid solutions, Solid State Ionics 113–115 (1998) 305–310.
[7] D.L. Maricle, T.E. Swarr, S. Karavolis, Enhanced ceria – a low-temperature SOFC electrolyte, Solid State Ionics 52 (1992) 173–182.
[8] C. Milliken, S. Guruswamy, A. Khandkar, Evaluation of ceria electrolytes in solid oxide fuel cells electric power generation, Journal of the Electrochemical Society 146 (1999) 872–882.
[9] P. Duran, C Moure, J.R. Jurado, Sintering and microstructural development of ceria-gadolinia dispersed powders, Journal of Materials Science 29 (1994) 1940–1948.
[10] K. Higashi, K. Sonoda, H. Ono, S. Sameshima, Y. Hirata, Synthesis and sintering of rare-earth-doped ceria powder by the oxalate coprecipitation method, Journal of Materials Research 14 (1999) 957967.
[11] D.A. Fumo, M.R. Morelli, A.M. Segadaes, Combustion synthesis of calcium aluminates, Materials Research Bulletin 31 (1996) 1243–1255.
[12] D.A. Fumo, J.R. Jurado, A.M. Segadaes, J.R. Frade, Combustion synthesis of iron-substituted strontium titanate perovskites, Materials Research Bulletin 32 (1997) 1459–1470.
[13] M.T. Colomer, D.A. Fumo, J.R. Jurado, A.M. Segadaes, Non-stoichiometric $La_{(1-x)}NiO_{(3-\delta)}$ perovskites produced by combustion synthesis, Journal of Materials Chemistry 9 (1999) 2505–2510.
[14] S. Gallini, J.R. Jurado, M.T. Colomer, Combustion synthesis of nanometric powders of $LaPO_4$ and Sr-substituted $LaPO_4$, Chemistry of Materials 17 (2005) 4154–4161.
[15] J.R. Jain, K.C. Adiga, V.R.Pai Verneker, A new approach to thermochemical calculations of condensed fuel-oxidizer mixtures, Combustion and Flame 40 (1981) 71–79.
[16] E. Chinarro, J.R. Jurado, M.T. Colomer, Synthesis of ceria-based electrolyte nanometric powders by urea-combustion technique, Journal of the European Ceramic Society 27 (2007) 3619–3623.
[17] T. Roisnel, J. Rodríguez-Carvajal, WinPLOTR: a windows tool for powder diffraction pattern analysis, Materials Science Forum 378–381 (2001) 118–123.
[18] X'Pert HighScore Plus, Version 2.2d, PANalytical BV, 2004.
[19] W. Shan, M. Luo, P. Ying, W. Shen, C. Li, Reduction property and catalytic activity of $Ce_{1-X}Ni_XO_2$ mixed oxide catalysts for $CH_4$ oxidation, Applied Catalysis A: General 246 (2003) 1–9.
[20] R.V. Wandekar, M. Ali, B.N. Wani, S.R. Bharadwaj, Physicochemical studies of NiO-GDC composites, Materials Chemistry and Physics 99 (2006) 289–294.
[21] B.L. Augusto, L.O.O. Costa, F.B. Noronha, R.C. Colman, L.V. Mattos, Ethanol reforming over Ni/CeGd catalysts with low Ni content, International Journal of Hydrogen Energy 37 (2012) 12258–12270.
[22] B. Solsona, P. Concepción, S. Hernández, B. Demicol, J.M. López-Nieto, Oxidative dehydrogenation of ethane over NiO–$CeO_2$ mixed oxides catalysts, Catalysis Today 180 (2012) 51–58.
[23] D. Hari Prasad, H.-I. Ji, H.-R. Kim, J.-W. Son, B.-K. Kim, H.-W. Lee, J.-H. Lee, Effect of nickel nano-particle sintering on methane reforming activity of Ni–CGO cermet anodes for internal steam reforming SOFCs, Applied Catalysis B: Environmental 101 (2011) 531–539.